BURNS, J. H. & GORDON, E. K. (1966). *Acta Cryst.* **20**, 135–138.
BUSING, W. R. (1972). *J. Chem. Phys.* **57**, 3008–3010.
CATLOW, C. R. A. & STONEHAM, A. M. (1983). *J. Phys. C*, **16**, 4321–4338.
COLLINS, D. M., MAHAR, M. C. & WHITEHURST, F. W. (1983). *Acta Cryst.* B**39**, 303–306.
DUNITZ, J. D., SCHWEIZER, W. B. & SEILER, P. (1983). *Helv. Chim. Acta*, **66**, 123–133.
HAHN, T. (1954). *Neues Jahrb. Mineral. Abh.* **86**, 1–65.
HESS, B., LIN, H. L., NIU, J. E. & SCHWARZ, W. H. E. (1993). *Z. Naturforsch. Teil A*. In the press.
HIRSHFELD, F. L. (1977). *Theor. Chim. Acta*, **44**, 129–138.
HIRSHFELD, F. L. & RABINOVICH, D. (1973). *Acta Cryst.* A**29**, 510–513.
LE PAGE, Y. & GABE, E. J. (1979). *Acta Cryst.* A**35**, 73–78.
MCGINNETY, J. A. (1973). *J. Chem. Phys.* **59**, 3442–3443.
MASLEN, E. N. & SPACKMAN, M. A. (1985). *Aust. J. Phys.* **38**, 273–287.
MATHIESON, A. MCL. (1982). *Acta Cryst.* A**38**, 378–387.
MATHIESON, A. MCL. (1984). *Acta Cryst.* A**40**, 355–363.
MATHIESON, A. MCL. (1988). *Aust. J. Phys.* **41**, 393–402.
SEILER, P. (1992). *Accurate Molecular Structures*, edited by A. DOMENICANO & I. HARGITTAI, pp. 170–198. Oxford Univ. Press.
SEILER, P. & DUNITZ, J. D. (1986*a*). *Helv. Chim. Acta*, **69**, 1107–1112.
SEILER, P. & DUNITZ, J. D. (1986*b*). *Helv. Chim. Acta.* **69**, 1187.
SEILER, P., SCHWEIZER, W. B. & DUNITZ, J. D. (1984). *Acta Cryst.* B**40**, 319–327.
STEWART, J. M. & HALL, S. R. (1990). Editors. *The XTAL System of Crystallographic Programs – User's Manual.* Univ. of Maryland, College Park, Maryland, USA.
STEWART, J. M., KRUGER, G. J., AMMON, H. L., DICKINSON, C. W. & HALL, S. R. (1972). The *XRAY*72 system – version of June 1972. Tech. Rep. TR-192. Computer Science Center, Univ. of Maryland, College Park, Maryland, USA.
ZACHARIASEN, W. H. (1926). *Nor. Geol. Tidsskr.* **9**, 65–73.

Acta Cryst. (1993). B**49**, 235–244

The Twin Structure of $La_2Ti_2O_7$: X-ray and Transmission Electron Microscopy Studies

BY HELMUT W. SCHMALLE, TIM WILLIAMS* AND ARMIN RELLER

Institute for Inorganic Chemistry, University of Zürich, Winterthurerstrasse 190, *CH*-8057 *Zürich, Switzerland*

ANTHONY LINDEN

Institute for Organic Chemistry, University of Zürich, Winterthurerstrasse 190, *CH*-8057 *Zürich, Switzerland*

AND J. GEORG BEDNORZ

IBM Research Division, Zürich Research Laboratory, CH-8803 *Rüschlikon, Switzerland*

(*Received* 15 *November* 1991; *accepted* 23 *September* 1992)

Abstract

$La_2Ti_2O_7$, $M_r = 485.613$, monoclinic, $P2_1$, $a = 7.812\,(2)$, $b = 5.5440\,(7)$, $c = 13.010\,(2)$ Å, $\beta = 98.66\,(1)°$, $V = 557.0\,(4)$ Å^3, $Z = 4$, $T = 298$ K, $D_x = 5.790$ Mg m^{-3}, λ(Mo $K\alpha$) = 0.71073 Å, $\mu = 17.86$ mm^{-1}, $F(000) = 856$. The crystals are twinned. The twin I and twin II intensities are superimposed in reciprocal-lattice layers with h even. The **a*** and **b*** axes of the twin components run antiparallel. The angle between $\mathbf{a}^*_{\text{twin I}}$ and $\mathbf{a}^*_{\text{twin II}}$ is 17.12°. The twinning operation has been identified to be a mirror plane perpendicular to the **c*** direction affecting only the oxygen positions in the structure: La and Ti atoms lie on an orthorhombic sublattice unchanged by the twinning. The structure refined on $|F|^2$ to $R = 0.040$, $wR = 0.085$ for 7972 observed reflections with $I > 3\sigma(I)$. The refinement was carried out by inclusion of the contributions from the two twin elements simultaneously, with the use of appropriate matrices to relate the atomic coordinates and reflection indices of each of the twin elements. The twin volume fraction was also refined and gave $\alpha = 0.1108\,(3)$ as the volume fraction of twin I. The enantiomorphs in twin I and twin II have been shown to be opposite by refinement, on $|F|$, of the enantiopole, or Flack's x, parameter against reflection data that had been separated into separate sets for each twin element. Subsequently, several refinements, on $|F|$, of the twinned data set with the use of all possible combinations of enantiomorphs of each twin element yielded the best R/wR values (0.040 and 0.056) when the twin components contained opposite enantiomorphs. The general features of the structure determined by Gasperin [*Acta Cryst.* (1975), B**31**, 2129–2130] could be confirmed: the twins comprise distorted (4 + 1 + 1) TiO_6 octahedra sharing vertices to form infinite perovskite-like layers three octahedra thick, bound by crystallographic

* Author to whom all correspondence should be addressed. Present address: JASCO International Co. Ltd., 4–21 Sennin-cho 2-chome, Hachioji City, Tokyo 193, Japan.

0108-7681/93/020235-10$06.00

shears in the **a** direction. La atoms occupy distorted perovskitic A sites and interlayer sites. $La_2Ti_2O_7$ is a member of an homologous series of $A_{n+1}B_{n+1}O_{3n+5}$ ($0 \le n \le \infty$) compounds with $n = 3$.

Introduction

$La_2Ti_2O_7$ belongs to a relatively small family of layered perovskite-related materials (Brandon & Megaw, 1970; Gasperin, 1975; Ishizawa, Marumo, Kawamura & Kimura, 1975). There are also a number of $A_2B_2O_7$ alkali-metal niobates and tantalates adopting this structure type [for example, $Ca_2Nb_2O_7$ (Brandon & Megaw, 1970) and $Sr_2Nb_2O_7$ (Ishizawa *et al.*, 1975)]; the optical and piezo- and ferroelectric properties of many of these phases are of interest (Nanamatsu, Kimura, Doi & Takahashi, 1971; Nanamatsu, Kimura & Kawamura, 1975). Gasperin, from her structure determination, indicated that $La_2Ti_2O_7$ is a member of an homologous series of layered structures built from {110} perovskitic slabs differing in thickness and bounded by crystallographic shears in the perovskite [100] direction. This compound is also a ferroelectric insulator with the highest known T_c of 1773 K (Nanamatsu, Kimura, Doi, Matsushita & Yamada, 1974). Adjacent slabs are offset from one another by half of one BO_6 octahedron height and the octahedron connectivity is broken at the shear interface. Perhaps surprisingly, very few members of this homologous series have been described, other than the $A_2B_2O_7$ phases. The $n = 1$ member structure of this series, $A_{n+1}B_{n+1}O_{3n+5}$, $0 \le n \le \infty$,* in which the $A_2B_2O_7$ materials are $n = 3$ members, is known in the fluorides ABF_4 (A = Ba, Sr; B = Zn, Ni, Fe) (von Schnering & Bleckmann, 1968) and the oxy-fluoride $NaNbO_2F_2$ (Andersson & Galy, 1969), which comprise crenellated layers of corner-connected BX_6 octahedra, one octahedron thick, bound by a zigzag layer of A cations. This structure is apparently unknown for a purely oxidic system. The $n = \infty$ end members have the perovskite structure, but otherwise the only ternary ($A + B + O$) structure in the family known as a bulk phase is that of $La_{10}Ti_{10}O_{34-y}$ (Lichtenberg, Widmer, Bednorz, Williams & Reller, 1991; Williams, Schmalle, Reller, Lichtenberg, Widmer & Bednorz, 1991), a reduced phase with the $n = 4$ structure type. Several higher members of the family have been reported in quarternary systems: $n = 4$ and 5 in the La–Ca–Ti–O system (Nanot, Queyroux & Gilles, 1973) and $n = 3$, $(NaCa)_2Nb_2O_7$, by Portier, Fayard, Carpy & Galy (1974).

* This representation of the homologous series is used here rather than the alternative, $A_nB_nO_{3n+2}$, $1 \le n \le \infty$, given by, for example, Carpy, Amestoy & Galy (1972) to show clearly the end members of this series: the minimal thickness $n = 0$ structure is then ABX_5 and $n = \infty$ the perovskite ABX_3.

There has been contention regarding the correct space group for $La_2Ti_2O_7$. One of the two single-crystal determinations for this phase suggested $P2_1$ (Gasperin, 1975), the other – performed at approximately the same time – suggested $Pna2_1$ (Scheunemann & Müller-Buschbaum, 1975), similar to the orthorhombic alkali-metal niobates. Recently, a convergent-beam electron diffraction (CBED) study of this material unambiguously showed that the correct choice at room temperature is $P2_1$ (Tanaka, Sekii & Ohi, 1985). However, at elevated temperatures both incommensurate and orthorhombic modifications of this structure exist; the former between 993 and 1053 K, and the latter, $Cmc2_1$ (Ishizawa, Marumo, Iwai & Kimura, 1977), from 1053 K to the melting point at about 2273 K. The isomorphous structures $Sr_2Ta_2O_7$ and $Sr_2Nb_2O_7$ undergo similar phase transitions (Yamamoto, Yagi, Honjo, Kimura & Kawamura, 1980). The study by Ishizawa *et al.* (1977) also noted the presence of twinning in this material. It was pointed out by Tanaka *et al.* (1985) that the earlier incorrect choice of orthorhombic symmetry was probably due to twinning. However, the correct structure determination by Gasperin (1975) was apparently performed for an untwinned crystal, prepared by growth in a PbO flux cooled from 1373 to 1073 K at 2 K h^{-1} and then presumably quenched rapidly through the orthorhombic-to-incommensurate and incommensurate-to-monoclinic transitions (Nanot *et al.*, 1973). It is also of interest that, uniquely, monoclinic $La_2Ti_2O_7$ has a cell with one axis double that observed in the alkali-metal niobates and tantalates, *i.e.* $a = 2 \times a_0$(cubic perovskite) $\simeq 7.8$ Å axis; the shortest axis is apparently common to all members of this structural family, $b = 2^{1/2}a_0$(cubic perovskite) $= 5.6$ Å.

Crystals of $La_2Ti_2O_7$ were examined by both high-resolution transmission electron microscopy (HRTEM) and single-crystal X-ray diffractometry in an attempt to clarify the twinning process that occurs both in this phase and in the homologous $La_{10}Ti_{10}O_{34}$ (Williams *et al.*, 1991). In the present paper the results of the X-ray structure determination based on the refinement on $|F|^2_{hkl}$ of both twin elements simultaneously are discussed with respect to refinements of separated reflection sets corresponding to twins I and II based on $|F|_{hkl}$ using Flack's x parameter to clarify possible inversion twinning in the structure. Electron microscopy results pertinent to the analysis of the twinning problem are also reported.

Experimental

Polycrystalline $La_2Ti_2O_7$ was synthesized by an infrared (IR) zone-melting technique, fully described

elsewhere (Williams *et al.*, 1991). Samples were melted from a ceramic starting (charge) rod of $La_2O_3 + 2TiO_2$, which we had prepared by mixing the weighed high-purity oxides in a suitable organic solvent and forming this paste into a rod of diameter about 5 mm, air drying and sintering in flowing purified $N_2 + O_2$ at 1473 K for about 12 h. The resulting material was then melted under flowing $N_2 + O_2$, typical growth rates being around 10–20 mm h^{-1}.

The zone-melted product was initially examined by optical microscopy. We prepared material for single-crystal X-ray studies by carefully crushing the product and selecting a damage-free fragment by optical methods and single-crystal X-ray photography. Intensity data were collected on an Enraf–Nonius CAD-4 four-circle diffractometer with graphite-monochromated Mo $K\alpha$ radiation ($\lambda = 0.71073$ Å).

We prepared samples for transmission electron microscope (TEM) studies by crushing pieces of the as-grown material in ethanol in an agate mortar and placing a drop of this suspension onto a holey-carbon TEM grid. The ETH-Zürich/Philips CM 30 analytical microscope fitted with a 'Super-Twin' high-resolution pole piece ($C_s = 1.2$ mm) and Gatan double-tilt low-background stage and operated at 300 kV was used for most of the TEM examinations. Additionally, a 200 kV JEOL 200 CX machine ($C_s = 1.2$ mm) at the University of Zürich and a 200 kV high-resolution electron microscope at the University of Cambridge (a specially modified JEOL 200 CX with $C_s = 0.5$ mm) were used for some examinations. As strong preferential cleavage of these materials was not a problem, we could readily examine several different zone-axial directions of the sample. Images at several different objective-lens excitations including the optimum ('Scherzer' focus) were taken and subsequently correlated with simulated images at known defocus. In one case, a wedge-shaped fragment cleaved at an angle off the [010] zone axis was found, which allowed observation of a range of defocus along the edge of a single-crystal fragment.

HRTEM image simulations were performed by the usual multislice method, with use of local Apple Macintosh II personal-computer versions of programs by Anstis (1985). Matrices of images in the [010] orientation were calculated for wide ranges of foil thickness, objective-lens focus, incident-beam convergence and chromatic defocus to permit comparison with the experimental images.

Results

The greater part of the zone-melted sample, approximately 30 mm in length and 4–5 mm in diameter, was transparent and of a light straw-yellow colour. This part had the appearance of being composed mainly of very large crystals several mm in length, as shown by faceting on the surface. The material could be cleaved into small regularly shaped platelets by careful crushing, and a number of these platelets were examined by optical microscopy to select one suitable for X-ray examination. The fragment considered below (of dimensions $0.33 \times 0.17 \times 0.15$ mm) gave a perfect exinction under crossed Nicol filters and was apparently free of damage.

Rotation photographs of the crystal mounted along the a axis showed an apparent cell in which the c axis was 26 Å and a characteristic distribution of strong intensities for layers with $h = 2n$ and weaker intensities when $h = 2n + 1$, in accordance with the diffraction pattern of a superstructure observed by Gasperin (1975). Furthermore, the Weissenberg diffraction pattern for layers $h = 2n + 1$ exhibited mostly weak reflections when $l = 2n$ ($2c = 26.0$ Å) and stronger reflections when $l = 2n + 1$, while in layers $h = 2n$ only strong reflections with $l = 2n$ were noted and, with a very few weak exceptions, reflections with $l = 2n + 1$ were absent, the exceptions probably owing to a disorder resulting from the tilting of oxygen octahedra in the structure. Attempts to refine the structure as a superstructure in the large cell with $2c = 26$ Å with the inclusion of twice the number of atoms, which had been transformed from the twinned refinement coordinates by (x, y, $z/2$) and (x, y, $1/2 + z/2$), were not successful as most of the anisotropic displacement parameters of the La, Ti and O atoms appeared to be non-positive-definite and reasonable convergence could not be achieved. Thus, a twinning effect in the **c*** direction was assumed rather than the presence of a superstructure. The twinning problem was confirmed by HRTEM and electron diffraction studies, and graphical considerations of the **a*c*** projections (see Figs. 3*b* and 4).

The estimation of twinning parameters for twins with exactly superimposed reciprocal lattices was discussed by Britton (1972) and in references cited therein, and a fundamental study on the characterization of twinning was produced by Santoro (1974). Twinning by merohedry and corresponding procedures for the X-ray crystal structure determination play an important role, as was pointed out by Catti & Ferraris (1976). A comprehensive article on crystal structure determination in the presence of twinning was presented by Jameson, Schneider, Dubler & Oswald (1982).

We have defined twin II to be represented by the stronger set of reflections of the unit cell a, b, c, β in the space group $P2_1$. The ab plane acts as a mirror, generating twin I and necessitating the collection of intensity data with the larger cell a, b, $2c$, β. More exact unit-cell parameters of the twin pair [a = 7.812 (2), b = 5.5440 (7), $2c$ = 26.020 (3) Å, β =

98.66 (1)°] were determined by least-squares refinement of the setting angles of 25 automatically centred reflections in the range $7.5 < \theta < 20.0°$. Intensities of 12440 reflections (including 126 standards) in the interval $-13 < h < 13$, $-9 < k < 9$, $0 < l < 45$ with θ between 1.0 and 38.0° were collected using the ω–2θ scan technique. The scan rate varied from 1.65 to 16.48° min^{-1}, the maximum measuring time being 50 s. Three standard reflections were monitored every 3 h measuring time and no loss of intensity was noted. Orientation was controlled every 400 reflections using four standard reflections. Lp and analytical absorption corrections (de Meulenaer & Tompa, 1965) ($\mu = 17.86\ mm^{-1}$) based on six indexed crystal faces and carefully measured distances between faces were applied to the measured data with use of the *TEXSAN* (Molecular Structure Corporation, 1989) program package. The transmission factors range from 0.103 to 0.219. The corrected data were then transferred to the *CRYSTALS* (Carruthers & Watkin, 1986) program system and data reduction continued to yield a unique set of reflections, in which the *hkl* and $h\bar{k}l$ reflections that are enantiomorphically sensitive were not averaged but still based on the unit cell in which the data were collected. The data were then reindexed to the small unit cell ($c = 13.01$ Å) in accordance with the recommended procedures for handling twinned structures given in the *CRYSTALS* manual. This required the indices for reflections that arose from either twin I or the superimposed reflections of both twins to be reindexed with use of the matrix (100, 010, $00\frac{1}{2}$), while those arising solely from twin II were reindexed with the matrix ($\bar{1}00$, 010, $\frac{1}{2}0\frac{1}{2}$). Reflection intensities did not need to be separated for the overlapping reflections as this is automatically handled by *CRYSTALS*.

Atomic coordinates from Gasperin (1975), with the *y* and *z* coordinates interchanged from those in the original work, were used as starting values for the refinement, which was carried out by employment of the contributions from both twin elements simultaneously, and minimization of $w(\Delta|F|^2)^2 = \sum_{hkl} w[(|F_o|^2) - (|F_c|^2)]^2$. The atomic positions were defined in the cell of twin I (as if it were untwinned) and the matrix ($\bar{1}00$, $0\bar{1}0$, $\frac{1}{2}01$) was used in the starting refinement to generate the corresponding atomic positions for twin II. (Subsequently the inverse of this matrix was employed when it was found necessary to refine the opposite enantiomorph for twin II – see below.) The nature of the procedure for the simultaneous refinement of twin elements with the *CRYSTALS* program is such that all of the parameters of twin I are explicity tied to the corresponding parameters of twin II. Thus, the molecular structure of twin II is identical with that of twin I, with the exception of the allowed change in the hand of the enantiomorph. The twin volume fractions were also refined with the total fraction restrained to 1.0. The volume fraction α for twin I finally refined to 0.1108 (3), in agreement with the estimated value $\alpha = 0.1185$, obtained from a comparison of equivalent nonoverlapping intensities I_I and I_{II} of the untwinned reflections [$h = 2n + 1$, $l = 2n$ for twin I with $c = 26.020$ (3) Å and $h = 2n + 1$, $l = 2n + 1$ for twin II]. The La, Ti and O atoms were refined with anisotropic displacement parameters. The final refinement on $|F|^2_{hkl}$ converged at $R/wR = 0.040/0.085$ with $(\Delta/\sigma)_{max} = 0.21$ for 7972 observed reflections with $I > 3\sigma(I)$ and 200 variable parameters. The weighting scheme employed used a 'robust resistant refinement' technique that is related to the Chebychev series (Rollett, 1965; Carruthers & Watkin, 1979). Essentially the weights are modified by a function expressing the confidence in $\Delta|F| = |F_o| - |F_c|$,

$$w = w'[1.0 - (\tfrac{1}{6}\Delta|F|/\Delta|F_{est}|)^2]^2$$

with

$$w' = 1.0/[A_0T_0'(F_c/F_{c\,max}) + A_1T_1'(F_c/F_{c\,max}) + \ldots + A_5T_5'(F_c/F_{c\,max})].$$

The maximum and minimum heights in the final difference electron density synthesis based on the $|F|^2_{hkl}$ refinement were 5.52 e $Å^{-3}$ [located 1.00 Å from O(3)] and -9.67 e $Å^{-3}$. The computation of difference electron density maps from twin refinements, especially when weak reflections are used, is described in the *CRYSTALS* manual as being a complex procedure, the results of which should be interpreted cautiously. Neutral atomic scattering factors were taken from *International Tables for X-ray Crystallography* (1974, Vol. IV, pp. 56–58, 99–102, 149–150). The refined atomic and isotropic displacement parameters are listed in Table 1.* The corresponding refinement on $|F|_{hkl}$ converged with $R/wR = 0.040$ and 0.056, where the weights were defined as $w = [\sigma^2(F)]^{-1}$.

Since the space group was polar, it was also necessary to ensure that the refined coordinates represented the correct enatiomorph in each of the twin elements. This was checked by two methods:

(*a*) repetition of the simultaneous refinement of both twins on F_{hkl}, with all permutations of enantiomorphs for twin I and twin II, and comparison of the resulting values of *R* and *wR*;

(*b*) division of the data into separate sets containing only the reflections for either twin I or twin II

* Lists of structure factors, anisotropic displacement parameters, and additional bond distances and angles have been deposited with the British Library Document Supply Centre as Supplementary Publication No. SUP 55710 (50 pp.). Copies may be obtained through The Technical Editor, International Union of Crystallography, 5 Abbey Square, Chester CH1 2HU, England.

Table 1. *Positional coordinates and equivalent isotropic displacement parameters U_{eq} for the twin pair of* $La_2Ti_2O_7$

$U_{eq} = (1/3)\sum_i \sum_j U_{ij} a_i^* a_j^* \mathbf{a}_i.\mathbf{a}_j$.

	x	y	z	U_{eq} (Å^2)
La(1)	0.27895 (3)	0.2565 (1)	0.11366 (2)	0.00500 (3)
La(2)	0.77399 (3)	0.2610 (1)	0.09946 (2)	0.00540 (3)
La(3)	0.35036 (3)	0.8092 (1)	0.39101 (2)	0.00940 (4)
La(4)	0.85240 (3)	0.8477 (1)	0.41598 (2)	0.00580 (3)
Ti(1)	0.0315 (1)	0.7661 (2)	0.11873 (5)	0.00440 (9)
Ti(2)	0.5273 (1)	0.7648 (2)	0.12005 (5)	0.00420 (9)
Ti(3)	0.0787 (1)	0.2973 (2)	0.32308 (5)	0.00520 (9)
Ti(4)	0.5834 (1)	0.3008 (2)	0.32632 (5)	0.00500 (9)
O(1)	0.7763 (4)	0.7983 (6)	0.1058 (3)	0.0089 (5)
O(2)	0.2737 (4)	0.6985 (6)	0.0934 (2)	0.0065 (4)
O(3)	0.0302 (4)	0.0247 (5)	0.0159 (2)	0.0069 (5)
O(4)	0.4776 (4)	0.0256 (5)	0.0180 (3)	0.0070 (4)
O(5)	0.0991 (4)	0.9683 (6)	0.2263 (3)	0.0087 (4)
O(6)	0.5141 (4)	0.9604 (6)	0.2295 (3)	0.0091 (4)
O(7)	0.0309 (5)	0.4588 (6)	0.1866 (2)	0.0071 (4)
O(8)	0.5612 (4)	0.4546 (5)	0.1860 (2)	0.0060 (4)
O(9)	0.0875 (5)	0.5593 (6)	0.4087 (3)	0.0085 (4)
O(10)	0.6161 (5)	0.5706 (6)	0.3991 (3)	0.0115 (6)
O(11)	0.1208 (4)	0.0778 (5)	0.4313 (2)	0.0053 (4)
O(12)	0.5992 (5)	0.0846 (5)	0.4394 (2)	0.0065 (4)
O(13)	0.3277 (4)	0.3247 (6)	0.3098 (2)	0.0087 (5)
O(14)	0.8255 (4)	0.2210 (6)	0.3042 (3)	0.0087 (4)

(with appropriate corrections of the intensities of overlapping reflections) and then refinement of the enantiopole, or Flack's x, parameter (Flack, 1983; Bernardinelli & Flack, 1987).

For method (*a*), the permutations were achieved by inversion of the signs of the matrix elements defining the coordinates of each twin element, one twin element at a time. The lowest values of R and wR were obtained when twin I was defined as the enantiomorph corresponding to the original coordinates (as given in Table 1) and twin II was defined with the use of the inverse of these coordinates.

For method (*b*), the efficacy of Flack's x refinement had been demonstrated impressively by Müller (1988). In this work, the x parameter refined to 0.03 (5) when the reflection set corresponding only to twin I was used and to 1.01 (3) when the reflection set corresponding to twin II was employed. This showed that the coordinates of twin II were inverted with respect to those of twin I, in agreement with the best refinement obtained using method (*a*). The x-parameter refinement is very stable and insensitive to systematic and absorption errors (Bernardinelli & Flack, 1987). As the e.s.d.'s of the x parameter for both twins appeared to be comparably small, the assignment of the enantiomorphs to both twins is unambiguous. The actual refinement results, on F, obtained with method (*b*) are as follows.

For the full-matrix least-squares refinement of the data corresponding to twin II according to method (*b*), 5893 reflections with $I > 3\sigma(I)$ and 200 variable parameters were used and all atoms were refined with anisotropic displacement parameters. The final R/wR values were 0.0355 and 0.0518 with $(\Delta/\sigma)_{max} = 0.02$. The maximum and minimum heights in the final difference electron density synthesis were 3.18 e Å^{-3} [1.12 Å from La(3)] and -8.67 e Å^{-3}.

The data corresponding to twin I (the weaker contributor to the intensities; $\alpha = 0.1108$) were refined in the same unit cell and under the same conditions (except that O atoms were refined only with isotropic displacement parameters) as the stronger diffracting component (twin II, above) using 5090 observed reflections and 130 variable parameters. The refinement was stopped at R/wR values of 0.0696 and 0.0878, with $(\Delta/\sigma)_{max}$ of 1.26 [O(1) y parameter]. The maximum and minimum heights in final difference electron density synthesis were 12.9 e Å^{-3} [0.52 Å from La(4)] and -21.3 e Å^{-3}. Weak intensities, disorder and possible absorption errors (the crystal faces were not perfectly grown) may explain the relatively poor R values and the high residual electron densities for twin I; however, the refined x parameter [$x = 0.03$ (5)] and its small estimated standard deviation (see Flack, 1983) confidently indicate the true enantiomorph for the twin I domains.

Discussion

Selected bond lengths and angles resulting from the simultaneous refinement of both twin elements are given in Table 2,* and the [100] and [010] projections of the structure are shown in Fig. 1, drawn with the aid of the plotting program *STRUPLO* (Fischer, 1985). Distances and angles were calculated with *ORFFE*3 (Busing, Martin, Levy, Brown, Johnson & Thiessen, 1971). As the two twins were refined in the same unit cell (although with different Miller indices after the *hkl* transformation), the twinning effect cannot be shown with use of the refined atomic coordinates of twin II. As already mentioned, except for the enantiomorph, the atomic positional parameters of twin II are identical with those of twin I, so that the resulting parameters listed in Tables 1 and 2 and used throughout the following discussion apply equally well in either twin domain.

The apical Ti—O distances vary between 1.768 (4) and 1.826 (4) Å and between 2.199 (3) and 2.288 (4) Å and the corresponding O atoms are O(3^{iii}) and O(5) for Ti(1), O(4^{iv}) and O(6) for Ti(2), O(5^{ii}) and O(9) for Ti(3), and O(6^{ii}) and O(10) for Ti(4) (see Table 2). The mean value of the equatorial Ti—O distances of the four independent octahedra was calculated as 1.963 (3) Å. The corresponding mean value of the short apical distance is 1.802 (4) Å and the long distance is 2.238 (4) Å. Thus the observed conformation is (4 + 1 + 1) distorted octahedral.

* See deposition footnote.

Table 2. *Bond distances* (Å) *and angles* (°) *for the twin pair of* $La_2Ti_2O_7$

TiO_6 octahedra bond distances

Ti(1)—O(1^{ix})	1.983 (3)	Ti(2)—O(1)	1.990 (3)
Ti(1)—O(2)	2.004 (3)	Ti(2)—O(2)	1.993 (3)
Ti(1)—O(3^{vii})	1.960 (3)	Ti(2)—O(4^{viii})	1.961 (3)
Ti(1)—O(3^{iii})	2.199 (3)	Ti(2)—O(4^{iv})	2.228 (4)
Ti(1)—O(5)	1.809 (4)	Ti(2)—O(6)	1.805 (4)
Ti(1)—O(7)	1.919 (3)	Ti(2)—O(8)	1.922 (3)
Ti(3)—O(5^{ii})	2.236 (4)	Ti(4)—O(6^{ii})	2.288 (4)
Ti(3)—O(7)	1.973 (3)	Ti(4)—O(8)	1.999 (3)
Ti(3)—O(9)	1.826 (4)	Ti(4)—O(10)	1.768 (4)
Ti(3)—O(11)	1.853 (3)	Ti(4)—O(12)	1.887 (3)
Ti(3)—O(13)	1.984 (3)	Ti(4)—O(13)	1.981 (3)
Ti(3)—O(14^{ix})	2.001 (3)	Ti(4)—O(14)	2.005 (3)

La—O coordination distances

La(1)—O(2)	2.464 (3)	La(2)—O(1^{ii})	2.567 (3)
La(1)—O(3)	2.510 (3)	La(2)—O(3^{viii})	2.749 (3)
La(1)—O(4)	2.485 (4)	La(2)—O(4)	2.729 (3)
La(1)—O(5^{ii})	2.701 (4)	La(2)—O(7^{viii})	2.415 (4)
La(1)—O(6^{ii})	2.740 (3)	La(2)—O(8)	2.397 (3)
La(1)—O(7)	2.543 (4)	La(2)—O(14)	2.643 (4)
La(1)—O(8)	2.516 (3)	La(2)—O(2^{i})	2.505 (4)
La(1)—O(13)	2.551 (3)	La(2)—O(3^{iv})	2.724 (3)
La(1)—O(1^{i})	2.832 (4)	La(2)—O(4^{iv})	2.729 (3)
La(1)—O(2^{ii})	3.105 (3)	La(2)—O(1)	2.980 (3)
La(1)—O(3^{iii})	3.108 (3)	La(2)—O(5^{v})	3.247 (3)
La(1)—O(4^{iv})	3.124 (4)	La(2)—O(6^{ii})	3.286 (4)
La(3)—O(5)	2.821 (3)	La(4)—O(9^{viii})	2.448 (4)
La(3)—O(6)	2.750 (4)	La(4)—O(10)	2.386 (4)
La(3)—O(9)	2.516 (4)	La(4)—O(11^{x})	2.437 (3)
La(3)—O(10)	2.451 (4)	La(4)—O(12^{vii})	2.431 (4)
La(3)—O(11^{vii})	2.448 (3)	La(4)—O(14^{vii})	2.520 (4)
La(3)—O(12^{vii})	2.478 (3)	La(4)—O(9^{vi})	2.545 (4)
La(3)—O(13)	2.882 (3)	La(4)—O(11^{vi})	2.471 (3)
La(3)—O(12^{vi})	2.512 (3)	La(4)—O(6)	3.366 (3)
La(3)—O(13^{vii})	3.043 (3)	La(4)—O(5^{viii})	3.418 (4)
La(3)—O(10^{vi})	3.068 (4)		

TiO_6 octahedra bond angles

O(5)—Ti(1)—O(7)	102.4 (1)	O(6)—Ti(2)—O(8)	101.9 (1)
O(5)—Ti(1)—O(2)	94.0 (2)	O(6)—Ti(2)—O(1)	101.0 (2)
O(5)—Ti(1)—O(3^{vii})	92.6 (1)	O(6)—Ti(2)—O(4^{vii})	93.6 (2)
O(5)—Ti(1)—O(1^{ix})	100.5 (2)	O(6)—Ti(2)—O(2)	94.3 (2)
O(5)—Ti(1)—O(3^{iii})	175.4 (1)	O(6)—Ti(2)—O(4^{iv})	175.8 (1)
O(7)—Ti(1)—O(2)	88.7 (2)	O(8)—Ti(2)—O(1)	93.1 (1)
O(7)—Ti(1)—O(3^{vii})	164.4 (1)	O(8)—Ti(2)—O(4^{vii})	164.0 (1)
O(7)—Ti(1)—O(1^{ix})	92.7 (2)	O(8)—Ti(2)—O(2)	88.8 (1)
O(7)—Ti(1)—O(3^{iii})	79.1 (1)	O(8)—Ti(2)—O(4^{iv})	79.2 (1)
O(2)—Ti(1)—O(3^{vii})	86.1 (1)	O(1)—Ti(2)—O(4^{vii})	88.0 (1)
O(2)—Ti(1)—O(1^{ix})	164.7 (2)	O(1)—Ti(2)—O(2)	163.9 (2)
O(2)—Ti(1)—O(3^{iii})	81.6 (1)	O(1)—Ti(2)—O(4^{iv})	83.0 (1)
O(3^{vii})—Ti(1)—O(1^{ix})	88.5 (1)	O(4^{vii})—Ti(2)—O(2)	85.9 (1)
O(3^{vii})—Ti(1)—O(3^{iii})	85.6 (1)	O(4^{vii})—Ti(2)—(4^{iv})	85.1 (1)
O(1^{ix})—Ti(1)—O(3^{iii})	83.7 (2)	O(2)—Ti(2)—O(4^{iv})	81.6 (1)
O(11)—Ti(3)—O(9)	94.2 (1)	O(10)—Ti(4)—O(12)	97.6 (2)
O(11)—Ti(3)—O(13)	93.0 (1)	O(10)—Ti(4)—O(14)	101.5 (2)
O(11)—Ti(3)—O(7)	165.9 (1)	O(10)—Ti(4)—O(8)	96.6 (2)
O(11)—Ti(3)—O(14^{ix})	90.8 (1)	O(10)—Ti(4)—O(13)	93.7 (2)
O(11)—Ti(3)—O(5^{ii})	82.7 (1)	O(10)—Ti(4)—O(6^{ii})	174.7 (2)
O(9)—Ti(3)—O(13)	92.6 (2)	O(12)—Ti(4)—O(14)	91.1 (2)
O(9)—Ti(3)—O(7)	99.9 (1)	O(12)—Ti(4)—O(8)	165.8 (1)
O(9)—Ti(3)—O(14^{ix})	100.9 (2)	O(12)—Ti(4)—O(13)	94.2 (2)
O(9)—Ti(3)—O(5^{ii})	173.5 (1)	O(12)—Ti(4)—O(6^{ii})	83.5 (1)
O(13)—Ti(3)—O(7)	86.7 (1)	O(14)—Ti(4)—O(8)	85.2 (1)
O(13)—Ti(3)—O(14^{ix})	165.7 (1)	O(14)—Ti(4)—O(13)	163.1 (1)
O(13)—Ti(3)—O(5^{ii})	81.9 (1)	O(14)—Ti(4)—O(6^{ii})	83.6 (1)
O(7)—Ti(3)—O(14^{ix})	86.3 (2)	O(8)—Ti(4)—O(13)	85.7 (1)
O(7)—Ti(3)—O(5^{ii})	83.3 (1)	O(8)—Ti(4)—O(6^{ii})	82.4 (1)
O(14^{ix})—Ti(3)—O(5^{ii})	84.9 (1)	O(13)—Ti(4)—O(6^{ii})	81.0 (1)

Symmetry operators: (i) $1-x, -0.5+y, -z$; (ii) $x, -1+y, z$; (iii) $-x, 0.5+y, -z$; (iv) $1-x, 0.5+y, -z$; (v) $1+x, -1+y, z$; (vi) $1-x, 0.5+y, 1-z$; (vii) $x, 1+y, z$; (viii) $1+x, y, z$; (ix) $-1+x, y, z$; (x) 1 + x, 1 + y, z.

The La—O coordination distances (Table 2) vary considerably: the resulting La-coordination spheres are complex and best understood with reference to the ball-and-stick representations in Fig. 2. La(1) and La(2) layers are coordinated by nine O atoms with La—O distances between 2.464 (3) and 2.832 (4) Å, and three additional La—O distances (see Table 2) range between 2.980 (3) and 3.286 (4) Å. The La atoms of the interplanar shear region are coordinated as follows: La(3) has eight nearest neighbour O atoms with distances between 2.448 (3) and 2.882 (3) Å, two other La—O lengths are 3.043 (3) and 3.068 (4) Å, while La(4) exhibits only seven short La—O distances between 2.386 (4) and 2.545 (4) Å and two long distances of 3.366 (3) and 3.418 (4) Å.

Both electron diffraction and HRTEM studies were carried out. HRTEM results are discussed in more detail elsewhere (Williams *et al.*, 1991) and with the exception of one HRTEM [010] image from a twin-containing fragment, only the diffraction results from the [010] zone axis are discussed here. However, the parallel HRTEM study gave no evidence for defects other than twin planes in the many fragments examined.

Fig. 3 shows [010] zone-axis electron diffraction patterns from (*a*) a perfect crystal and (*b*) a twinned crystal. The patterns could be indexed for both twins with use of a projection of the previously reported cell, $a \simeq 7.8$, $c \simeq 13.0$ Å, $\beta \simeq 98.6°$ with appropriate transformation of the cell for the second twin (Fig. 3*b*). Fig. 4 shows the pattern of Fig. 3(*b*) schematically and it can be seen that there is a very pronounced (centred) orthogonal subcell ($a \simeq 3.9$, $c \simeq 26.0$ Å) in this projection, resulting from the cation sublattice of the structure. Many crystals were examined in this orientation and either one of the twin domains predominated or only one twin domain was observed. In the HRTEM image of Fig. 5(*a*), two twin planes parallel with the {001} layers of the structure can be seen if the image is viewed at a shallow angle in the direction indicated by the large arrow. These were the only twin domains visible in the thin regions of this fragment examined at high resolution, suggesting that the volume of the 'minority' twin is much smaller than the other – in agreement with the intensities in the corresponding selected-area diffraction pattern (Fig. 3*b*). The twin planes are only readily visible in the thicker parts of the crystal away from the edge, as an abrupt change

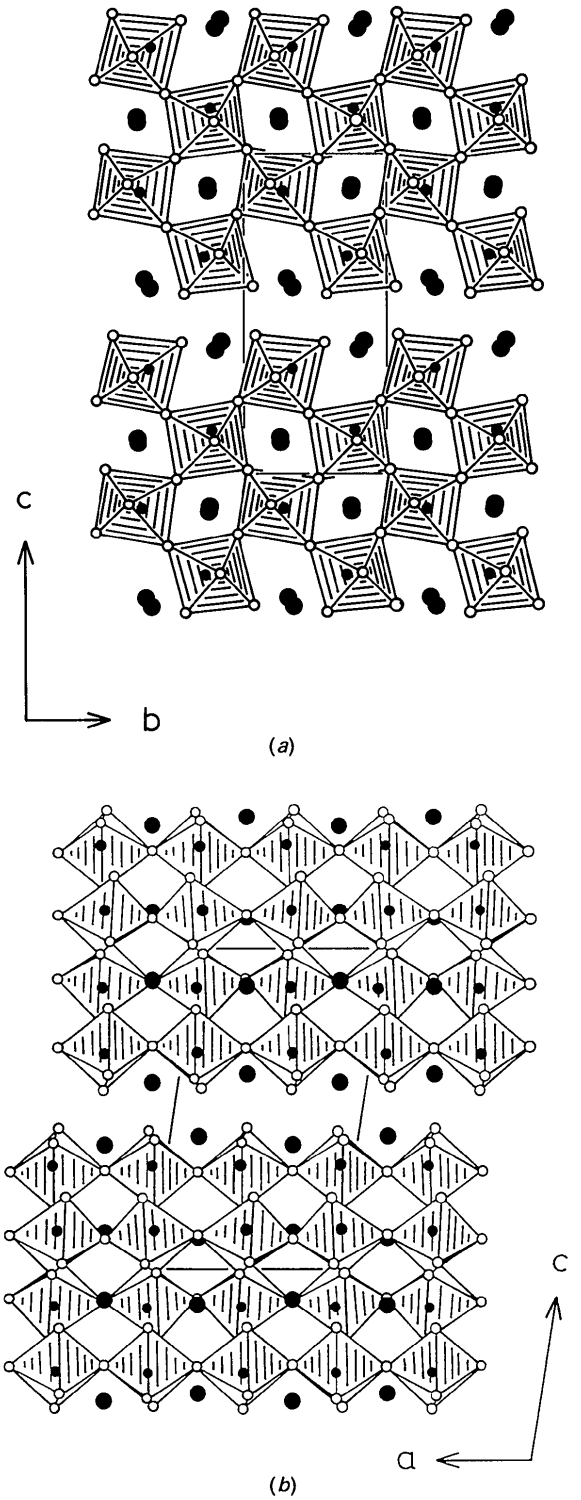

Fig. 1. Polyhedral representations of the structure of $La_2Ti_2O_7$ in (*a*) the *bc* and (*b*) the *ac* projections. Two slabs of the structure are shown in each representation, with large and small filled circles representing the La and Ti atoms, respectively, and small open circles representing the O atoms. The monoclinic true cells are outlined.

in the directions of rows of strong white fringes: those normally at an angle of about 98° to the layers change within the minor twin region to run at 180 − 98 = 82° to the layers, hence the visual features here correspond with the mirror twinning observed by electron and single-crystal X-ray diffraction. In Fig. 5(*b*) an enlargement of the twinned region at about Scherzer focus illustrates the change in the cell across the twin planes (arrowheads): the $\beta = 98°$ cell is outlined for both twins I and II, but with a shift in the origin for clarity.

To confirm the TEM observations, images were calculated by the usual multislice method, with the use of the atomic coordinates from the X-ray refinement of the twin pair. Other parameters used (spherical aberration coefficient C_s, chromatic defocus, beam convergence) were appropriate to the Philips CM 30 microscope. Matrices of images in the [010] orientation were calculated for appropriate values of specimen thickness, objective-lens defocus, beam convergence *etc.* The projected atomic potentials were also output to locate atom positions in the images. The inset in Fig. 5(*b*) is a calculated image for a 47 Å thick foil at 400 Å underfocus. The images closely match, indicating the general correctness of the imaging conditions assumed. Our simulations confirmed that, with use of the identical choice of unit cell and orientation, the two twins (or their enantiomorphs) cannot be distinguished by their image contrast alone. However, the change of cell orientation across the twin plane in the experimental image clearly indicates its location.

There appears to be no strong structural reason favouring either of the two octahedral layer confor-

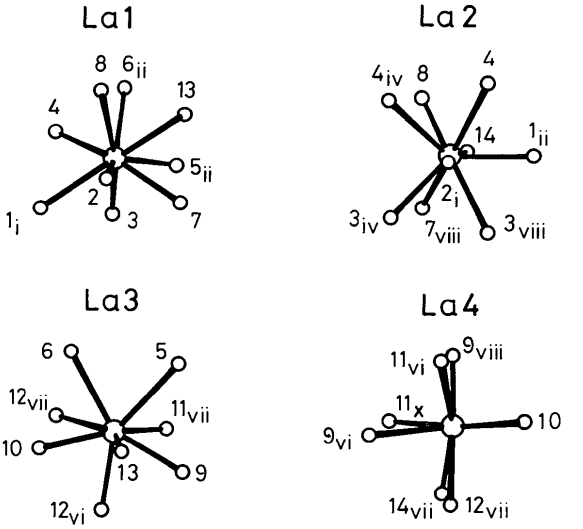

Fig. 2. Ball-and-stick perspective illustration of the four different La—O coordinations in $La_2Ti_2O_7$. The O-atom numbering corresponds with that in Table 2.

mations, although it is then perhaps surprising that the twins do not occur in approximately equal volumes in every crystal fragment. During the transition from the high-temperature orthorhombic $Cmc2_1$ structure through the intermediate incommensurate phase, it is likely that the orientations of the tilted TiO_6 octahedra in the bulk material are 'uncommitted' to either twin; that is, there is an averaged median orientation above 1053 K in the orthorhombic phase region or a temperature-related orientation within the incommensurate phase region from 1053 to 993 K. When the monoclinic phase forms at 993 K there is a transition to one or other maximally tilted orientation resulting in the appearance of twin bands noted earlier (Tanaka *et al.*, 1985) and here. Alternatively, both twin types of the monoclinic modification may be represented by slightly different structural forms in the incommensurate phase region, with the transition at 1053 K, not 993 K, determining the final twin distribution at room temperature. In this latter case a TEM study at elevated temperatures within the incommensurate phase field could conceivably image these two regions separately by their different contrast.

Bond-length and valence considerations suggest that the coordination environments around the Ti and La ions are more complex than those suggested by the apparent nearest neighbour O-atom arrangements. Ti(1) and (2) are apparently 'correctly' bonded; valences s calculated from the parameters of Brown & Altermatt (1985) and the Ti—O and La—O distances of this work give 4.056 for Ti(1) and 4.039 for Ti(2), but 4.107 for Ti(3) and 4.103 for Ti(4) are somewhat anomalous. The averaged Ti valence is 4.076.

Similarly, the coordination spheres around La(1) and La(2) are probably complete with fewer nearest neighbour O atoms than those noted above. For La(1), a distorted bis-disphenoidal, coordination is suggested, with one additional 'capping' bond to La(2). For La(1) and La(2), bond-strength sums give s = 3.049 and 2.995 with nine nearest neighbours. In the interplanar shear region La(3) is somewhat under-bonded with 2.913 electrons (8 + 2 nearest neighbours in a distorted rhombic configuration), whereas La(4) is over-bonded by inclusion of all

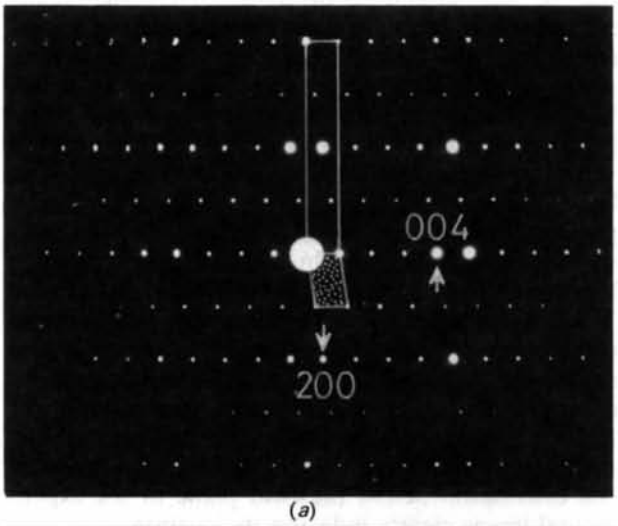

(*a*)

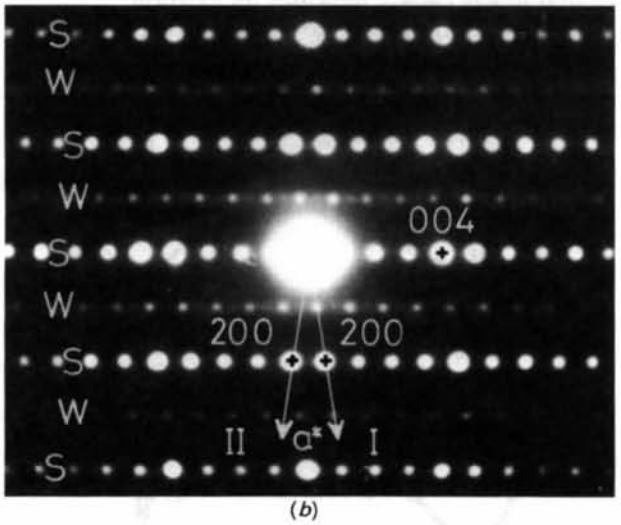

(*b*)

Fig. 3. (*a*) Selected-area [010] zone-axis electron difraction pattern from (*a*) an untwinned and (*b*) a twinned crystal fragment. (*a*) The projection of the reciprocal net (corresponding to the cell parameters 7.8 × 13 Å) is stippled and the centred orthogonal reciprocal subcell (3.9 × 26 Å) is outlined. (*b*) Alternate reciprocal-space rows S and W are strong and weak rows from (primarily) the cation sublattice and the oxygen sublattice, respectively. In contrast with (*a*), reflections from twin types I and II are visible on the weak rows $h0l$, $h = 2n + 1$.

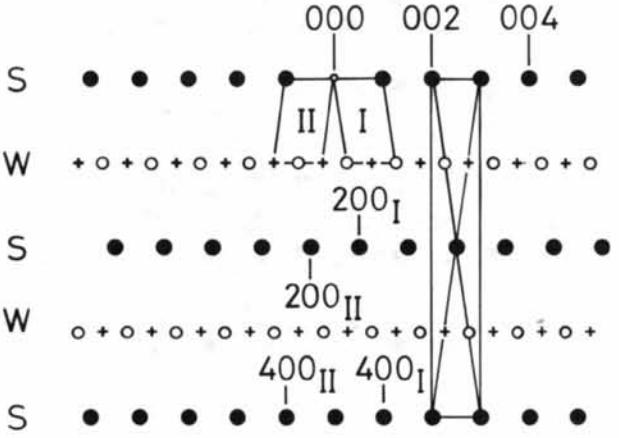

Fig. 4. Schematic illustration of the diffraction pattern in Fig. 3(*b*). Large filled circles represent common or untwinned reflections. Small open circles are reflections from twin I only and small crosses represent twin II reflections only. Rows S and W have the same meaning as in Fig. 3(*b*). Reciprocal unit meshes for twins I and II are outlined separately, as is the centred orthogonal subcell corresponding to the untwinned cation arrays.

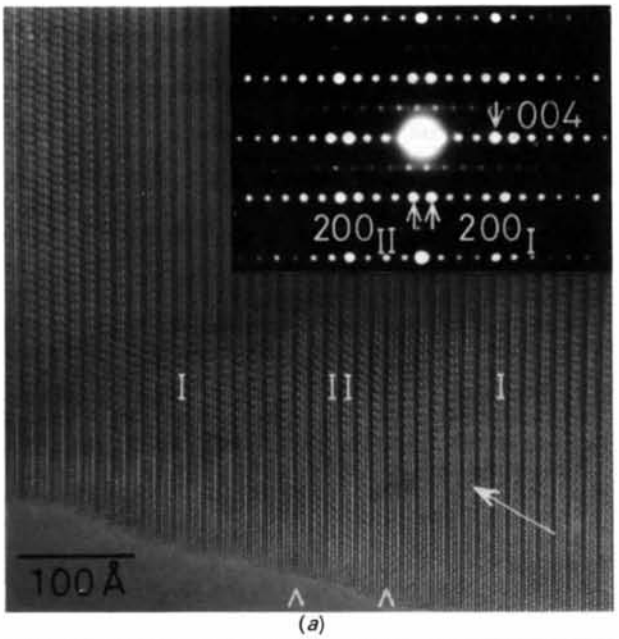

(*a*)

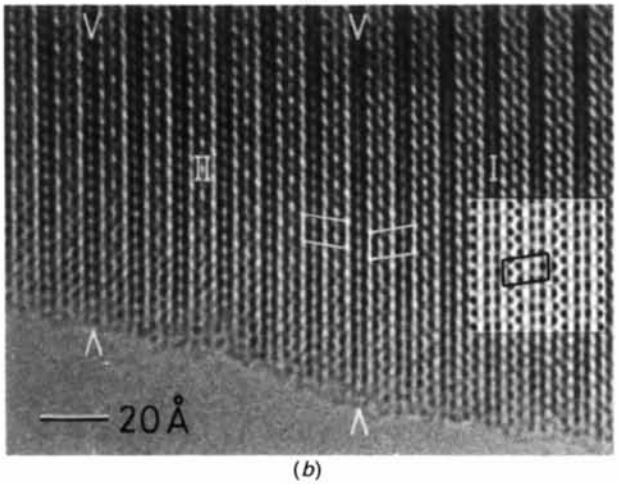

(*b*)

Fig. 5. (*a*) High-resolution [010] zone-axis image of $La_2Ti_2O_7$ from a twinned crystal fragment taken at 300 kV. The crystal has cleaved at an angle from {010} and hence the defocus varies across the crystal, from nearly Gaussian (zero) on the left to nearly Scherzer defocus on the right. The two twin boundaries in this fragment are indicated by arrows at the bottom of (*a*), the majority twin type II flanking the thin slab of twin I. If (*a*) is viewed along the plane of the page in the direction arrowed the twinned region is clearly seen. The corresponding selected-area diffraction pattern is inset with reflections of type 200 for each twin (I and II) marked. (*b*) Enlargement of the central part of (*a*) showing the change in cell orientation across the twin boundary. Two unit cells are outlined either side of the central twin plane (arrowed). The doubling of the basic structural repeat of ~3.9 Å to give the true cell $a \simeq 7.8$ Å is seen as a slight intensity modulation of the white spots running along the layers [vertical in (*b*)], more so in the thicker parts of the crystal. At the thin edge, black dots correspond to Ti and La atoms: zigzag rows of dots are the sheared interlayer region and the tramline rows (dark stripes at the top) the perovskitic slabs. A calculated image for a foil 47 Å thick at 400 Å underfocus (close to Scherzer condition) with a cell outlined to correspond with twin type I is inset.

seven La—O bonds shorter than 2.6 Å (*i.e.* by omission of the two distant bonds at about 3.4 Å) with $s = 3.246$. Removal of the longest bond at ~2.6 Å leads to the more reasonable s value of 2.797, although these La atoms are now coordinated by only six O atoms arranged approximately octahedrally. Whilst La(3) has a valence of 2.823 with nine neighbouring O atoms, La(4) still has the unusual configuration of six or seven O atoms and respective valencies of 2.797 or 3.246.

The averaged valence for the La ions, with La(1) and La(2) in nine, La(3) in ten and La(4) in six coordination, is 2.892. With seven O atoms around La(4) this increases to 3.004. All the La atoms in this structure are in a much lower coordination state than in the ABO_3 perovskite structure. The data of Maclean, Ng & Greedan (1979) for the structure of $LaTiO_3$ suggest that eight nearest neighbour O atoms (La—O between 2.45 and 2.773 Å) surround the A atoms in a rhombic prismatic configuration with four next nearest neighbour O atoms (3.054 to 3.309 Å, 'capping bonds') completing the La coordination. For all 12 bonds, $s = 2.792$, although the contribution of delocalized electrons to the La valence in this metallic material is unknown. Satisfactory La—O bonding in insulating $La_2Ti_2O_7$ might be explained on the basis of charge transfer between the two interplanar La ions and possibly between the inter- and intraplanar La atoms.

The authors wish to thank Professor H. R. Oswald for continuous support of this project and Professor John Günter for fruitful discussions. TW warmly thanks Professor G. Kostorz of ETH Zürich for his kind hospitality and provision of electron microscope facilities, and Dr D. Jefferson of the University of Cambridge for access to the Cambridge HREM. TW is grateful to the Swiss National Science Foundation for financial support (grant No. 2.838–085). Gratitude is expressed to the Co-editor Professor H. Burzlaff and for the referee's suggestions concerning the twinning problem of the X-ray analysis. HWS kindly thanks Professor O. Jarchow of the University of Hamburg for fruitful discussions about the enantiomorph twinning.

References

ANDERSSON, S. & GALY, J. (1969). *Acta Cryst.* B**25**, 847–850.

ANSTIS, G. R. (1985). Private communication.

BERNARDINELLI, G. & FLACK, H. D. (1987). *Acta Cryst.* A**43**, 75–78.

BRANDON, J. K. & MEGAW, H. D. (1970). *Philos. Mag.* **21**, 189–194.

BRITTON, D. (1972). *Acta Cryst.* A**28**, 296–297.

BROWN, I. D. & ALTERMATT, D. (1985). *Acta Cryst.* B**41**, 244–247.

BUSING, W. R., MARTIN, K. O., LEVY, H. A., BROWN, G. M., JOHNSON, C. K. & THIESSEN, W. A. (1971). *ORFFE*3. *A Fortran Function and Error Program.* Report ORNL-TM-306 (revised). Oak Ridge National Laboratory, Tennessee, USA.

CARPY, A., AMESTOY, P. & GALY, J. (1972). *C. R. Acad. Sci. Sér. C*, **275**, 833–835.
CARRUTHERS, J. R. & WATKIN, D. L. (1979). *Acta Cryst.* A**35**, 698–699.
CARRUTHERS, J. R. & WATKIN, D. L. (1986). *CRYSTALS*. Issue 9. Chemical Crystallography Laboratory, Oxford, England.
CATTI, M. & FERRARIS, G. (1976). *Acta Cryst.* A**32**, 163–165.
FISCHER, R. X. (1985). *J. Appl. Cryst.* **18**, 258–262.
FLACK, H. D. (1983). *Acta Cryst.* A**39**, 876–881.
GASPERIN, M. (1975). *Acta Cryst.* B**31**, 2129–2130.
ISHIZAWA, N., MARUMO, F., IWAI, S. & KIMURA, M. (1977). *Annu. Meet. Mineral. Soc. Jpn*, p. 68.
ISHIZAWA, N., MARUMO, F., KAWAMURA, T. & KIMURA, M. (1975). *Acta Cryst.* B**31**, 1912–1915.
JAMESON, G. B., SCHNEIDER, R., DUBLER, E. & OSWALD, H. R. (1982). *Acta Cryst.* B**38**, 3016–3020.
LICHTENBERG, F., WIDMER, D., BEDNORZ, J. G., WILLIAMS, T. & RELLER, A. (1991). *Z. Phys.* B**82**, 211–216.
MACLEAN, D. A., NG, H.-N. & GREEDAN, J. E. (1979). *J. Solid State Chem.* **30**, 35–44.
MEULENAER, J. DE & TOMPA, H. (1965). *Acta Cryst.* **19**, 1014–1020.
Molecular Structure Corporation (1989). *TEXSAN. Single-Crystal Structure Analysis Package*. Version 5.0. MSC, 3200 Research Forest Drive, The Woodlands, TX 77381, USA.
MÜLLER, G. (1988). *Acta Cryst.* B**44**, 315–318.
NANAMATSU, S., KIMURA, M., DOI, K., MATSUSHITA, T. & YAMADA, Y. (1974). *Ferroelectrics*, **8**, 511–513.
NANAMATSU, S., KIMURA, M., DOI, K. & TAKAHASHI, M. (1971). *J. Phys. Soc. Jpn*, **30**, 300–301.
NANAMATSU, S., KIMURA, M. & KAWAMURA, T. (1975). *J. Phys. Soc. Jpn*, **38**, 817–824.
NANOT, M., QUEYROUX, F. & GILLES, J. C. (1973). *C. R. Acad. Sci. Sér. C*, **277**, 505–507.
PORTIER, R., FAYARD, M., CARPY, A. & GALY, J. (1974). *Mater. Res. Bull.* **9**, 371–378.
ROLLETT, J. S. (1965). *Computing in Crystallography*, edited by J. S. ROLLETT, p. 40. Oxford: Pergamon.
SANTORO, A. (1974). *Acta Cryst.* A**30**, 224–231.
SCHEUNEMANN, K. & MÜLLER-BUSCHBAUM, H.-K. (1975). *J. Inorg. Nucl. Chem.* **37**, 1879–1881.
SCHNERING, H. G. VON & BLECKMANN, P. (1968). *Naturwissenschaften*, **55**, 342–343.
TANAKA, M., SEKII, H. & OHI, K. (1985). *Jpn. J. Appl. Phys.* **24**(Suppl. 2), 814–816.
WILLIAMS, T., SCHMALLE, H., RELLER, A., LICHTENBERG, F., WIDMER, D. & BEDNORZ, G. (1991). *J. Solid State Chem.* **93**, 534–548.
YAMAMOTO, N., YAGI, K., HONJO, G., KIMURA, M. & KAWAMURA, T. (1980). *J. Phys. Soc. Jpn*, **48**, 185–191.

Acta Cryst. (1993). B**49**, 244–254

Phasons Modulate the Atomic Debye–Waller Factors in Incommensurate Structures: Experimental Evidence in $ThBr_4$ at 55 K*

BY G. MADARIAGA, J. M. PÉREZ-MATO AND I. ARAMBURU

Departamento de Física de la Materia Condensada, Facultad de Ciencias, Universidad del País Vasco, Apartado 644, 48080 *Bilbao, Spain*

(*Received* 13 *July* 1992; *accepted* 25 *September* 1992)

Abstract

The incommensurate displacive structure of β-$ThBr_4$ at 55 K has been determined from a neutron diffraction data set including main reflections and first-order satellites. The superspace group is $P^{I4_1/amd}_{s\,1\,s1}$. Final agreement factors are 0.0193, 0.0186 and 0.045 for all, main and satellite reflections, respectively. It is shown that the effect of phasons on the atomic Debye–Waller factors can be quantified by two additional structural parameters: the modulus $\beta^{Br}_{11,2}$ and the phase $\chi^{Br}_{11,2}$ of a second harmonic that spatially modulates the temperature factors of Br atoms. Results are in good agreement, within the resolution of the experimental data, with the theoretically expected value for $\chi^{Br}_{11,2}$. Crystal data for the average structure: $M_r = 551.65$, tetragonal, $I4_1/amd$, $a = 8.919\ (1)$, $c = 7.902\ (1)$ Å, $V = 628.6\ (2)$ Å^3, $Z = 4$, $D_x = 5.82$ Mg m^{-3}, $\lambda = 0.84$ Å, wavevector $\mathbf{q} = 0.32\mathbf{c}^*$.

* Preliminary results of this work were presented at the International Workshop on Methods of Structural Analysis of Modulated Structures and Quasicrystals, Lekeitio, Spain, May 1991.

1. Introduction

The experimental detection of phase-fluctuation effects on the temperature factors of incommensurate (IC) structures is still unresolved in structural determination. Indeed, the quantitative evaluation of these effects has been a subject of controversy in some descriptions of IC structures. The theoretical formulation of the influence of these low-frequency excitations on the Debye–Waller factors has followed a path of increasing complexity from the simplest Overhauser (1971) approach to its final recently established general form (Currat & Janssen, 1987; García, Pérez-Mato & Madariaga, 1989; Pérez-Mato & Madariaga, 1990; Pérez-Mato, Madariaga & Elcoro, 1991).

Overhauser's fomulation of the phason Debye–Waller factor (PDWF) introduces a surprising overall factor, $\exp(-\frac{1}{2}n^2\langle\delta\varphi^2\rangle)$, dependent on the mean-

0108-7681/93/020244-11$06.00